Relay-aided Slotted Aloha for UAV-Assisted Mixed UOWC-RF Systems

Tijana Devaja, Srdjan Sobot, Milica Petkovic, Marko Beko, Dejan Vukobratovic

***Abstract*—In this paper, we design and analyse a relay-aided Slotted ALOHA solution for uplink random access in a mixed underwater optical wireless communications (UOWC)-radio frequency (RF) system. The first uplink phase represents the UOWC transmission between underwater devices and the floating buoys, which act as surface relays. The second uplink phase is performed by radio-frequency (RF) communications between buoys and an unmanned Aerial Vehicle (UAV) hovering over the water surface. Analytical expression for end-to-end throughput is derived, and utilized to analyse performance dependence on the UOWC and RF channel conditions, as well as UAV position. The performance improvement due to employment of relaying is observed under various channel and traffic conditions.**

***Index Terms*—Slotted ALOHA (SA), Throughput, underwater optical wireless communications (UOWC), Unmanned Aerial Vehicles (UAV).**

I. Introduction

Growth of Internet of Things (IoT) connections is projected to increase from 13.2 billion in 2022 to 34.27 billion in 2028 [1]. The 5G and beyond-5G communications systems face the challenge of ensuring reliable connectivity with high energy and spectral efficiency to accommodate extreme IoT connection densities [1]–[3]. Over the past decades, IoT systems have undergone extensive research, design, and development, finding extensive applications in diverse range of use cases across various domains such as industry [4], smart transportation [5], smart energy [6], smart cities [7], healthcare [8], and others.

Given that approximately 70% of the Earth's surface is covered by water, the scope of IoT applications has broadened to encompass underwater environments [9]. The underwater IoT constitutes an intelligent network of interconnected underwater objects, including sensor nodes, autonomous underwater vehicles (AUVs), boats, divers, and other. Underwater IoT system performance are dependent on specific characteristics of the underwater medium, resulting in different designs and channel models compared to the classical IoT systems. Although acoustic communications have primarily been deployed as wireless technology within underwater IoT [10], underwater optical wireless communications (UOWC) have been considered as a potential alternative to fulfill specific demands of underwater medium (UOWC) [11]–[14]. The OWC employment within underwater IoT applications is justified due to distinctive optical signal propagation through water media, leading to the low power consumption, security, high bandwidth and low cost of UOWC systems [14]–[17]. In underwater environments, the establishment of connectivity for short and sporadic data transmissions is essential due to potentially vast population of IoT devices. As underwater IoT transmission often involves short packets and unpredictable device activity, Slotted ALOHA (SA) can be employed as a suizable random access scheme in IoT system [18], [19]. As far as we know, the SA based UOWC system within IoT applications has been analysed only recently in [20], [21].

Low-cost and highly mobile unmanned aerial vehicles (UAVs) have been considered for various applications, such as environmental monitoring, 3D connectivity with terrestrial cellular or satellite networks, delivery services, disaster management, search and rescue missions. Due to fast deployment and line-of-sight (LoS) connections without complex infrastructure requirements, UAVs have been utilized for remote sensing and relaying systems, in order to collect data from multiple sensors through ground-to-air links [22]–[25]. Recently, UAV-based mixed UOWC-RF have been proposed as a promising way to provide connection between underwater devices and communication network via hovering UAVs [26]–[28].

Inspired by aforementioned, the aim of the paper is to design and analyse UAV-based mixed UOWC-RF system while considering the SA policy for both UOWC and RF links. The system under investigation represents the SA based uplink transmission from underwater IoT users to the floating buoys at water surface which act as relays that forward the packets to the hovering UAV via Nakagami-distributed RF links. Proposed system setup is inspired by the one presented in [29], related to satellite communications, where the data is transmitted from ground users to the satellites, which then relay the packets to the central ground station, while SA is adopted as a random access protocol. Differently from [29], which assumes simple on-off fading channels for both links, we consider medium-specific environments for both uplinks, while the erasure of packets is dependent on either UOWC or RF channel models. More precisely, mixed

T. Devaja, S. Sobot, M. Petkovic and D. Vukobratovic are with University of Novi Sad, Faculty of Technical Science, 21000 Novi Sad, Serbia (e-mails: tijana.devaja@uns.ac.rs; srdjansobot@live.com; milica.petkovic@uns.ac.rs; dejanv@uns.ac.rs).

M. Beko is with Instituto de Telecomunicações, Instituto Superior Técnico, Universidade de Lisboa, Lisbon, Portugal, and Copelabs, Universidade Lusofona de Humanidades e Tecnologias, Lisbon, Portugal, (e-mail: beko.marko@gmail.com).

This work has received funding from the Horizon 2020 research and innovation staff exchange grant agreement No 101086387, and from the Science Fund of the Republic of Serbia, grant number 6707, REmote WAter quality monitoRing anD IntelliGence – REWARDING. This work has been supported by the Secretariat for Higher Education and Scientific Research of the Autonomous Province of Vojvodina through the project "Visible light technologies for indoor sensing, localization and communication in smart buildings" (142-451-2686/2021). This publication was based upon work from COST Action NEWFOCUS CA19111, supported by COST (European Cooperation in Science and Technology)

exponential–generalized gamma (EGG) distribution, proposed in [11], is used to characterize turbulence-induced fading in UOWC system, while considering presence of air bubbles and temperature gradient for fresh and salty water. In UOWC systems, understanding the characteristics of the water medium is crucial for accurate channel modeling. The bubble level is used to measure the level of turbulence which can significantly affect the propagation of optical signals through water. These factors can cause scattering, absorption, and refraction of the light signals, leading to signal attenuation, distortion, and reduced transmission range. In presented analysis, we adopt combined model of mixture EGG distributed turbulence model and pointing errors [12], [13] to model the UOWC environment, while the RF links are modeled by Nakagami-*m* distribution as a general model convenient for both LoS and non-LoS transmissions [30]. Following the mathematical analysis presented in [29], the end-to-end throughput is derived, which is further used to observe the trade-offs between the UAV-based mixed UOWC-RF system throughput performance and both UOWC and RF system parameters.

The rest of the text is organized as follows. Section II defines the system model, while in Section III we provide the throughput performance analysis. Numerical results are given in Section IV and Section V concludes the paper.

II. System Model

The two-tier topology of the UAV-assisted mixed UOWC-RF system is considered in the paper, as presented in Fig. 1. The overall uplink transmission includes two hops. The first one is related to the uplink UWOC scenario that consists of the signal transmission from underwater IoT devices to floating buoys, acting as K decode-and-forward (DF) based relays. As shown in Fig. 1, all buoys are located on the water surface, being equally spaced along the circumference of a circle with radius R. The second hop represents the uplink RF transmission from the buoys to the hovering UAV, which is positioned at a normal distance L from the water surface. All buoys are thus equidistant from the UAV. The SA medium access protocol is adopted for both transmissions [31].

A. The first link: Underwater OWC uplink transmission

The first hop represents an uplink UOWC communication. The underwater IoT devices transmit data packets in an uncoordinated fashion to K DF-based relays, i.e., floating buoys, placed on the water surface. They are equipped with OWC transmitters, such as LEDs or laser diode, which employ the intensity modulation with on-off keying in order to satisfy non-negative constraint. All buoys at the water surface contain the OWC receivers (photodetectors) where direct detection and optical-to-electrical signal is performed.

The optical signal is transmitted through a turbulent channel. After optical-to-electrical conversion, the received signal at the OWC relay can be represented as:

$$y = P_{opt}\eta I x + n \tag{1}$$

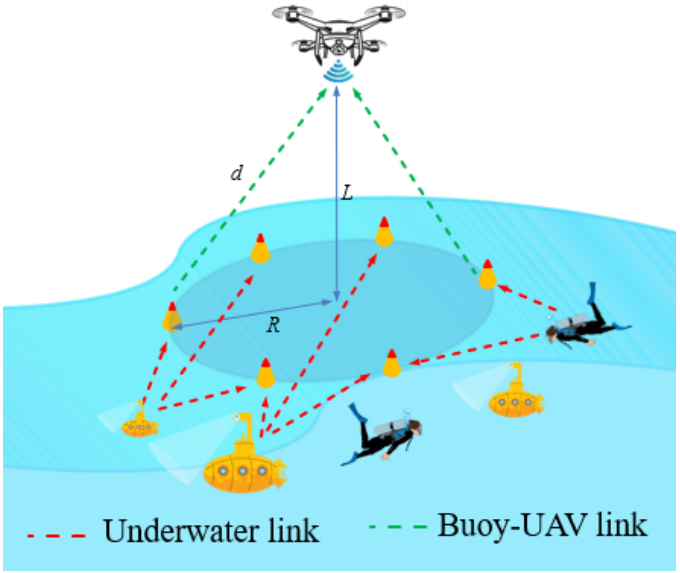

Fig. 1. Considered scenario.

where x is the signal transmitted by the active user, P_{opt} Popt represents the transmit optical power, η denotes the optical-to-electrical conversion coefficient, and I is the normalized irradiance due to underwater turbulence mixture of EGG fading [1] and pointing errors. Gaussian white noise n is modeled as a zero-mean Gaussian random variable with variance N_0.

The instantaneous signal-to-noise ratio (SNR) for the UOWC link can be defined as:

$$\gamma_1 = \frac{I^2}{\mathbb{E}[I]^2}\mu_1, \tag{2}$$

where $\mathbb{E}[\cdot]$ denotes the expectation operation, and μ_1 is the average electrical SNR defined as:

$$\mu_1 = \frac{(P_{opt}\eta\,\mathbb{E}[I])^2}{N_0}, \tag{3}$$

related to the average SNR as:

$$\bar{\gamma_1} = \frac{\mu_1\,\mathbb{E}[I^2]}{\mathbb{E}[I]^2}. \tag{4}$$

The UOWC link is affected by both the underwater optical turbulence characterized by the mixture EGG distribution and the pointing errors [12], [13]. The n-th moment of I is derived in [13] as:

$$\mathbb{E}[I^n] = w\frac{(\lambda_1 A_0)^n n!\xi^2}{n+\xi^2} + (1-w)\frac{(bA_0)^n\Gamma(a+\frac{n}{c})\xi^2}{\Gamma(a)(n+\xi^2)}. \tag{5}$$

[1]Note that fading in underwater communication can be quite significant due to various factors like multipath propagation, absorption, attenuation, scattering and environmental variability, which can be overcome using mitigation techniques, such as adaptive modulation and coding, diversity techniques, and channel equalization.

TABLE I
PARAMETERS OF THE EGG DISTRIBUTION FOR DIFFERENT BUBBLE LEVELS BL (L/MIN) FOR FRESH WATER AND SALTY WATER [11]

Salinity	BL	ω	λ	a	b	c
Salty Water	4.7	0.2064	0.3953	0.5307	1.2154	35.7368
Salty Water	7.1	0.4344	0.4747	0.3935	1.4506	77.0245
Salty Water	16.5	0.4951	0.1368	0.0161	3.2033	82.1030
Fresh Water	4.7	0.2190	0.4603	1.2526	1.1501	41.3258
Fresh Water	7.1	0.3489	0.4771	0.4319	1.4531	74.3650
Fresh Water	16.5	0.5117	0.1602	0.0075	2.9963	216.8356

The probability density function (PDF) for the instantaneous SNR γ_1 affected by the mixture EGG fading turbulence and the pointing errors is formulated as [12, eq. (3)]:

$$f_{\gamma_1}(\gamma) = \frac{w\xi^2}{2\gamma} G_{1,2}^{2,0}\left(\frac{1}{\lambda A_0}\left(\frac{\gamma}{\rho_1}\right)^{\frac{1}{2}} \middle| \begin{matrix} \xi^2+1 \\ 1,\xi^2 \end{matrix}\right) + \frac{(1-w)\xi^2}{2\Gamma(a)\gamma} G_{1,2}^{2,0}\left(\frac{1}{b^c A_0^c}\left(\frac{\gamma}{\rho_1}\right)^{\frac{c}{2}} \middle| \begin{matrix} \frac{\xi^2}{c}+1 \\ a, \frac{\xi^2}{c} \end{matrix}\right), \quad (6)$$

where $G_{p,q}^{m,n}(\cdot\,|\,\cdot)$ is the Meijer's *G*-function [32, (9.301)], $\Gamma(z)$ defines the Gamma function [32, (8.31)], and $\rho_1 = \bar{\gamma_1}/\,\mathbb{E}[I]^2$.

The parameters w, λ, a, b, and c characterize the turbulence properties associated with the mixture EGG distribution, which fluctuate depending on factors such as water salinity and bubble level (BL). The values of these parameters are defined in [11], and outlined in Table I. The parameters A_0 and ξ are related to pointing errors. According to [12, eq. (4)], the cumulative density function (CDF) of γ_1 is defined as:

$$F_{\gamma_1}(\gamma) = w\xi^2 G_{2,3}^{2,1}\left(\frac{1}{\lambda_1 A_0}\left(\frac{\gamma}{\rho_1}\right)^{\frac{1}{2}} \middle| \begin{matrix} 1,\xi^2+1 \\ 1,\xi^2,0 \end{matrix}\right) + \frac{(1-w)\xi^2}{c\Gamma(a)} G_{2,3}^{2,1}\left(\frac{1}{b^c A_0^c}\left(\frac{\gamma}{\rho_1}\right)^{\frac{c}{2}} \middle| \begin{matrix} 1, \frac{\xi^2}{c}+1 \\ a, \frac{\xi^2}{c},0 \end{matrix}\right). \quad (7)$$

B. The second link: Buoys-UAV uplink transmission

The second link of mixed UWOC-RF scenario given in Fig. 1 represents the RF uplink channel between buoys and the hovering UAV. After packets are correctly received, each buoy, acting as a DF relay, re-encodes and forwards data packets to the UAV. We assume that no buffering is done at the relays, leading to the case when the packets are either forwarded to the UAV in the subsequent slot, or they are discarded.

The instantaneous SNR over RF link can be defined as:

$$\gamma_2 = h^2 \mu_2, \quad (8)$$

where h is the signal fading amplitude over RF link modeled by Nakagami-*m* distribution, while the average SNR is:

$$\mu_2 = \frac{P_t g_{\mathrm{UAV}}}{\sigma_R^2}, \quad (9)$$

where P_t denotes the RF transmitted power, g_{UAV} represents the average power gain of the RF link, and σ_R^2 is the the additive white Gaussian noise variance. If distance between each buoy and UAV is denoted by d ($d^2 = R^2 + L^2$), the average power gain can be determined as [33]:

$$g_{\mathrm{UAV}} = G_0 d^{-2} = \frac{G_0}{R^2 + L^2}, \quad (10)$$

where G_0 denotes the channel power gain at the reference distance $R_0 = 1$ m.

Each buoy-to-UAV RF channel is modeled by independent and identical distributed (i.i.d.) Nakagami-*m* distribution. The PDF and the CDF of the instantaneous SNR of buoy-to-UAV RF link are given as follows [34]:

$$f_{\gamma_2}(\gamma) = \frac{m^m \gamma^{m-1}}{\mu_2^m \Gamma(m)} e^{-\frac{m\gamma}{\mu_2}}, \quad (11)$$

$$F_{\gamma_2}(\gamma) = 1 - \frac{\Gamma\left(m, \frac{m\gamma}{\mu_2}\right)}{\Gamma(m)}, \quad (12)$$

where m is the Nakagami-*m* fading parameter, and $\Gamma(\cdot,\cdot)$ represents the Incomplete Gamma function [32, (8.350.2)].

III. THROUGHPUT PERFORMANCE ANALYSIS

In the proposed system, we assume that both uplinks apply the classical SA protocol. In underwater system, the average number of packets sent per slot is defined as the channel load G [pk/slot]. In this analysis, the number of underwater IoT devices transmitting the data over a slot is modeled a Poisson-distributed random variable U with intensity G as:

$$\Pr\{U = u\} = \frac{G^u e^{-G}}{u!}. \quad (13)$$

Since classical SA policy is employed, the packet will be recovered and forwarded to UAV only if a single packet reaches the buoy relay during a slot. In other words, collisions are destructive, and the buoy relay will recover the data only if one of the transmitted packets is successfully received.

Presented analysis in the first underwater system assumes that any packet at the buoy relay will be erased if the instantaneous SNR over UOWC link, γ_1, defined in (2), is lower than previously determined threshold γ_{th_1}. Under asymptotic criteria, the error probability of data packet transmission $\epsilon(\gamma_1)$ as a function of channel parameter γ_1 is approximated with a step function, i.e., $\epsilon(\gamma_1) = 1$ if $\gamma_1 < \gamma_{\mathrm{th}}$, otherwise, $\epsilon(\gamma_1) = 0$. We define ϵ_1 as a probability that any packet at the buoy relay is erased if its instantaneous SNR is lower than γ_{th_1}. Consequently, a packet at the buoy relay arrives with probability $1 - \epsilon_1$. Since the underwater IoT device-to-buoy relay link is assumed to be previously defined UOWC channel, the probability ϵ_1 is determined as the CDF defined in (7), i.e., $\epsilon_1 = F_{\gamma_1}(\gamma_{\mathrm{th}_1})$. The probability that successful reception of data conditioned on $U - u$ transmission occurs can be determined as [29]:

$$\mathrm{p}_u := u(1-\epsilon_1)\epsilon_1^{u-1}. \quad (14)$$

After removing the conditioning, the average throughput experienced at each of the K buoy relays is equal to the throughput of a SA link with erasures [29], which is derived as follows:

$$T_{\text{uowc}} = \sum_{u=1}^{\infty} \frac{G^u e^{-G}}{u!} \mathrm{p}_u = G(1-\epsilon_1) e^{-G(1-\epsilon_1)}. \quad (15)$$

In next uplink RF communication system, all of K buoy relays intend to transmit the recovered packets to the UAV. The SA approach is again adopted for the RF link, so that the data will be decoded if only one packet successfully reaches a UAV within a slot. As defined in Section II, all RF channels between buoy relays and UAV are modeled as i.i.d. Nakagami-*m* fading links. Similarly as in the UOWC system, ϵ_2 defines the erasure probability of the packet at UAV. Thus the probability that data packet at the UAV will be erased can be determined based on the CDF defined in (12) as $\epsilon_2 = F_{\gamma_2}(\gamma_{\text{th}_2})$, where γ_{th_2} is previously determined threshold.

Following the approach given in [29], the end-to-end throughput of the considered system is derived as follows. Assuming $U = u$ underwater IoT are active and send the packets, the overall probability that the buoy successfully decodes one of the transmitted packets, forwards it to UAV, and that the packet is not erased over the RF link, can be defined as:

$$\mathrm{q}_u := \mathrm{p}_u(1-\epsilon_2). \quad (16)$$

Adopted SA policy considers that the packet will be decoded at UAV only if a single packet is received unfaded. In other words, the packet will be decoded only if its SNR is greater then threshold γ_{th_2}, and the rest of transmitted packets are erased due to failure to meet this condition. This is expressed through the conditional binomial probability, given $U = u$, as:

$$\mathrm{z}_u := K \mathrm{q}_u (1-\mathrm{q}_u)^{K-1}. \quad (17)$$

After removing the conditioning on z_u, the end-to-end throughput for the UOWC-RF system is determined as [29]:

$$T = \sum_{u=1}^{\infty} \frac{G^u e^{-G}}{u!} \mathrm{z}_u = \sum_{u=1}^{\infty} \frac{G^u e^{-G}}{u!} K \mathrm{q}_u (1-\mathrm{q}_u)^{K-1}. \quad (18)$$

In order to avoid throughput presentation in terms of infinite series, derivation presented in [29, Appendix A] is adopted, resulting in the closed-form expression of end-to-end throughput given by [29] :

$$T = \sum_{i=0}^{K-1} (-1)^i K \binom{K-1}{i} e^{-G} \times \left(\frac{(1-\epsilon_1)(1-\epsilon_2)}{\epsilon_1} \right)^{i+1} H_{i+1}\left(G\epsilon_1^{i+1}\right), \quad (19)$$

where the ancillary function is defined as:

$$H_m(x) = \begin{cases} e^x, & m = 0 \\ x \sum_{l=0}^{m-1} \binom{m-1}{l} H_l(x), & m \geq 1 \end{cases}. \quad (20)$$

IV. Numerical Results

By using derived analytical expressions for the end-to-end throughput, numerical results are presented in this section. The proposed scenario is analyzed by adopting the following values for the UOWC parameters: the conversion efficiency is $\eta = 0.4$, the transmitted optical power $P_{opt} = 100$ mW, the noise power spectral density $N_0 = 10^{-21}$ W/Hz. Table I represents the adopted values of the UOWC parameters [11]. Regarding the UAV-based links, the following parameters are assumed: the transmitted optical power $P_t = -3.01$ dBm, the noise variance $\sigma_R^2 = -90$ dBm, the channel power gain at the reference distance $G_0 = -30$ dB [33]. The SNR thresholds are assumed to be the same for both UOWC and RF uplinks, i.e., $\gamma_{\text{th}_1} = \gamma_{\text{th}_2} = 5$ dB.

Fig. 2 depicts the end-to-end throughput dependence on the channel load considering: i) different number of employed relays, ii) different salinity of water, iii) different level of bubbles. In Fig. 2, maximal throughput can be noted which is achieved at an optimal value of the channel load. This optimal value of channel load varies for different air bubbles level, but it is independent on the number of employed relays. With greater number of the buoy relays denoted by K, the optimal channel load stays the same, but the maximum achievable throughput is getting higher, proving that the utilization of greater number of relays will improve system performance. Beyond the optimal point, further increases in channel load lead to decreased throughput. This decrease happens because in areas of heavy load, more users contend for the same relays, increasing the likelihood of collisions. For lower channel load G, denser air bubbles leads to performance deterioration, which changes after optimal channel load, i.e., the type of air bubbles level has an important impact on the system performance. In our analysis, we examine both salty and fresh water scenarios. The impact of water salinity on the performance of the UOWC system appears to be relatively minor compared to

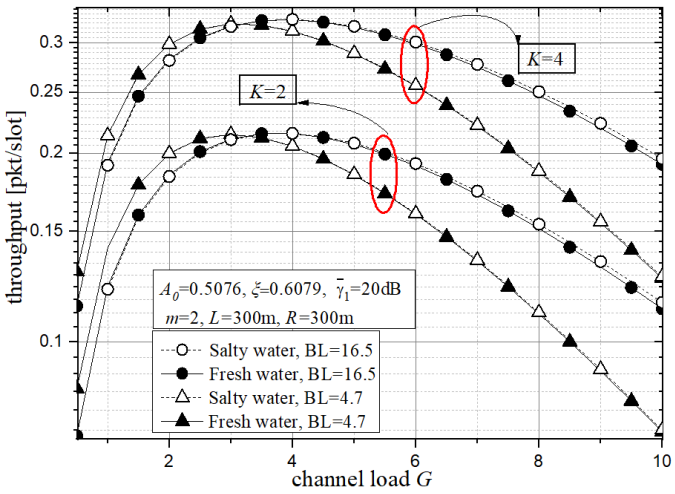

Fig. 2. End-to-end throughput vs. channel load for different number of relays, bubble levels and salinity of water.

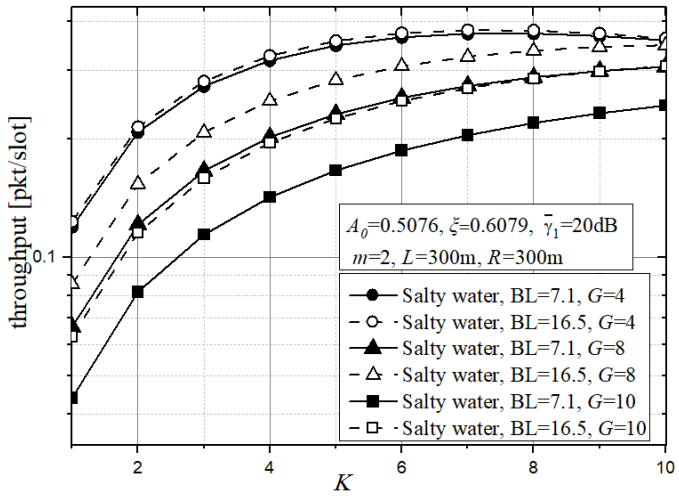

Fig. 3. End-to-end throughput vs. number of relays.

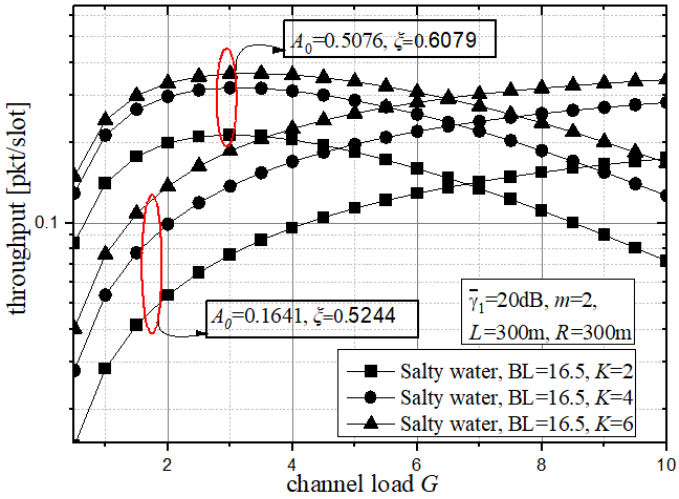

Fig. 4. End-to-end throughput vs. channel load for different values of pointing errors strength.

the influence of air bubbles. The presence of bubbles leads to rapid fluctuations in intensity, which significantly affect system performance. This suggests that while water salinity has a minor effect, it is overshadowed by the more severe impact of air bubbles on system performance, which should be taken into consideration during system design.

Fig. 3 presents how the increase in the number of relays affects the system throughput for different load conditions in salty water. For lower channel load, adding the relays will cause throughput performance improvement until some point. After this optimal number of relays, appending more relays will cause slight system performance impairment since most of them will overpower the threshold and there will be a lot of unfaded packets at the relays. The collisions will occur resulting in lower throughput. For higher G, more underwater users access the shared medium, thus greater number of relays reflects in the performance improving.

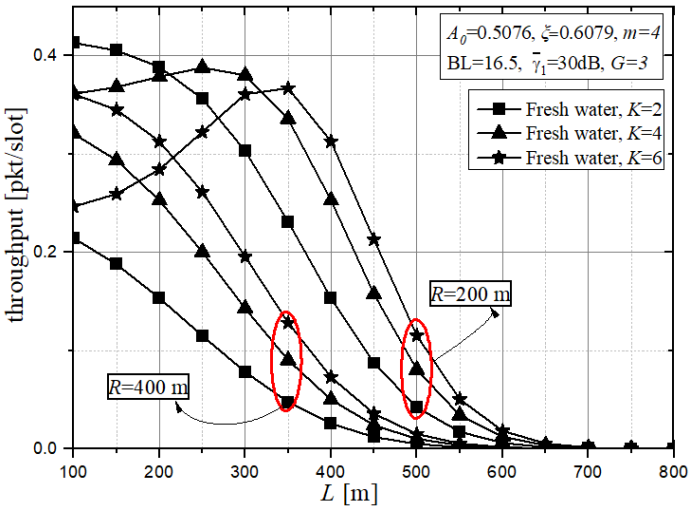

Fig. 5. End-to-end throughput vs. drone height.

In Fig. 4 we examine the effect of the pointing errors on the performance of the overall link. We study the case of salty water with BL=16.5 for different number of relays. The parameters A_0 and ξ determine the pointing errors impact. From Fig. 4 it can be observed that parameters $A_0 = 0.5076$, $\xi = 0.6079$ (weaker pointing errors) gives better results than the parameters $A_0 = 0.1641$, $\xi = 0.5244$ (stronger pointing errors) when channel load is lower. With channel load increase, the number of active users in UOWC system is greater, thus the worse underwater channel conditions, i.e., stronger pointing errors, will results in the performance improvement. This is justified by the fact that large number of users will be affected by pointing errors effect, and the packet will be erased, which reduces the overall channel load at the second RF system.

Fig. 5 shows throughput dependence on the UAV height L, considering different number of relays and different radius of the circle buoys are positioned. As it expected, when radius R is greater ($R = 400$ m in this case), increasing of L will lead to system performance degradation due to more severe path loss. Adding more buoy relays will improve the system performance. If the radius of the circle is lower (e.g. $R = 200$ m), the maximal value of the throughput is noticed for optimal value of L. When both L and R are short distances, overall path loss between buoys and UAV will be weak, and the most transmitted packets will not be erased. Collisions will happen at UAV which result in lower overall throughput. If L is increasing, distance between buoys and UAV will be larger and number of erased packet will be greater. At optimal distance L maximal throughput will be achieved. With increasing of L after optimal value, system performance is worsening. The optimal values of L vary for different number of relays. To conclude, design of proposed system should pay attention on both UAV and buoys positions in order to achieve maximal number of recovered packets in overall system.

V. Conclusion

In this paper, we have analysed a relay-aided SA mixed UOWC-RF system. The first part of uplink transmission represents the UOWC environment, where the underwater devices perform transmission to the multiple buoy relays by SA approach. The second part refers to the SA-based RF transmission from the buoy relays to hovering UAV. Considering different characteristics of both underwater and UAV-based RF channel conditions, the packet erasure probabilities are determined and utilized to calculate the end-to-end throughput. Based on presented analysis, numerical results are obtained and utilized to discuss the throughput behavior of the mixed UOWC-RF system. It was concluded that UOWC channel conditions influence the system performance, which should be taken into consideration during the system design. Additionally, positions of UAV and buoys should be also considered during the system design in order to get the insight about the maximal achievable throughput. Also, the achieved throughput gain due to adding of relays is dependent on both the OWC and RF channel conditions.

References

[1] https://www.ericsson.com/en/reports-and-papers/mobility-report/dataforecasts/iot-connections-outlook

[2] H. Tataria, et al., "6G wireless systems: Vision, requirements, challenges, insights, and opportunities," *Proc. IEEE*, vol. 109, no. 7, 2021.

[3] N. H. Mahmood, et al., "White paper on critical and massive machine type communication towards 6G," arXiv preprint arXiv:2004.14146.

[4] B. S. Khan, S. Jangsher, A. Ahmed, and A. Al-Dweik, "URLLC and eMBB in 5G Industrial IoT: A Survey," *IEEE Open J. Commun. Soc.*, vol. 3, pp. 1134-1163, 2022.

[5] B. Jan, H. Farman, M. Khan, M. Talha, and I. U. Din, "Designing a Smart Transportation System: An Internet of Things and Big Data Approach," *IEEE Wirel. Commun.*, vol. 26, no. 4, pp. 73-79, 2019.

[6] G. Bedi, G. K. Venayagamoorthy, R. Singh, R. R. Brooks, and K. C. Wang, "Review of Internet of Things (IoT) in Electric Power and Energy Systems," in *IEEE Internet Things J.*, vol. 5, no. 2, pp. 847-870, 2018.

[7] A. S. Syed, D. Sierra-Sosa, A. Kumar, and A. Elmaghraby, "IoT in smart cities: A survey of technologies, practices and challenges," *Smart Cities,* vol. 4, no. 2, pp. 429-475, 2021.

[8] F. Nausheen and S. H. Begum, "Healthcare IoT: Benefits, vulnerabilities and solutions," in *Proc. IEEE ICISC*, Coimbatore, India, pp. 517-522, 2018.

[9] M. C. Domingo, "An overview of the internet of underwater things," *J. Netw. Comput.*, vol. 35, no. 6, pp. 1879-1890, 2012.

[10] M. Chitre, S. Shahabudeen, L. Freitag, and M. Stojanovic, "Recent advances in underwater acoustic communications & networking," in *Proc. OCEANS 2008*, Quebec City, QC, Canada, pp. 1-10, 2008.

[11] E. Zedini, H. M. Oubei, A. Kammoun, M. Hamdi, B. S. Ooi, and M.-S. Alouini, "Unified statistical channel model for turbulence-induced fading in underwater wireless optical communication systems," *IEEE Trans. Commun.*, vol. 67, no. 4, pp. 2893-2907, 2019.

[12] L. Yang, Q. Zhu, S. Li, I. S. Ansari and S. Yu, "On the Performance of Mixed FSO-UWOC Dual-Hop Transmission Systems," *IEEE Wirel. Commun. Lett.*, vol. 10, no. 9, pp. 2041-2045, 2021.

[13] S. Li, L. Yang, D. B. Costa, and S. Yu, "Performance analysis of UAV-based mixed RF-UWOC transmission systems," *IEEE Trans. Commun.*, vol. 69, no. 8, pp. 5559-5572, 2021.

[14] M. Elamassie, F. Miramirkhani and M. Uysal, "Channel modeling and performance characterization of Underwater Visible Light Communications," in *Proc. ICC Workshops*, 2018.

[15] M. F. Ali, D. N. K. Jayakody and Y. Li, "Recent trends in Underwater Visible Light Communication (UVLC) systems," *IEEE Access*, vol. 10, pp. 22169-22225, 2022.

[16] N. Saeed, A. Celik, T. Y. Naffouri and M. S. Alouini, Underwater optical wireless communications, networking, and localization: A survey," *Ad Hoc Netw.*, vol. 94, 2019.

[17] S. Arnon, "Underwater optical wireless communication network," *Opt. Eng.*, vol. 49, no. 1, 2010.

[18] F. Clazzer, A. Munari, G. Liva, F. Lazaro, C. Stefanovic, and P. Popovski, "From 5G to 6G: Has the time for modern random access come?" in *Proc. 1st 6G summit*, Levi, Finland, 2019.

[19] S. A. Tegos, P. D. Diamantoulakis, A. S. Lioumpas, P. G. Sarigiannidis, and G. K. Karagiannidis, "Slotted ALOHA with NOMA for the next generation IoT," *IEEE Trans. Commun.*, vol. 68, no. 10, pp. 6289–6301, 2020.

[20] C. T. Nguyen, M. T Nguyen, and V. V. Mai, "Underwater optical wireless communication-based IoUT networks: MAC performance analysis and improvement," *Opt. Switch. Netw.*, vol. 37, 2020.

[21] M. Petkovic et al., "Slotted Aloha for Optical Wireless Communications in Internet of Underwater Things," *IEEE WOCC*, Newark, NJ, USA, pp. 1-5, 2023.

[22] T. Andre et al., "Application-driven design of aerial communication networks," *IEEE Commun. Mag.*, vol. 52, no. 5, pp. 129–137, 2014.

[23] D. W. Matolak and R. Sun, "Air–Ground Channel Characterization for Unmanned Aircraft Systems—Part I: Methods, Measurements, and Models for Over-Water Settings," textitIEEE Trans. Veh. Technol., vol. 66, no. 1, pp. 26-44, Jan. 2017.

[24] R. Sun and D. W. Matolak, "Air–Ground Channel Characterization for Unmanned Aircraft Systems Part II: Hilly and Mountainous Settings," *IEEE Trans. Veh. Technol.*, vol. 66, no. 3, pp. 1913-1925, 2017.

[25] D. W. Matolak and R. Sun, "Air–Ground Channel Characterization for Unmanned Aircraft Systems—Part III: The Suburban and Near-Urban Environments," in *IEEE Trans. Veh. Technol.*, vol. 66, no. 8, pp. 6607-6618, 2017.

[26] H. Lei, Y. Zhang, K.-H. Park, I. S. Ansari, G. Pan, and M.-S. Alouini, "Performance analysis of dual-hop RF-UWOC systems," *IEEE Photon. J.*, vol. 12, no. 2, pp. 1–15, 2020.

[27] S. Li, L. Yang, D. B. Da Costa, and S. Yu, "Performance analysis of UAV-based mixed RF-UWOC transmission systems," *IEEE Trans. Commun.*, vol. 69, no. 8, pp. 5559–5572, 2021.

[28] P. Agheli, H. Beyranvand and M. J. Emadi, "UAV-Assisted Underwater Sensor Networks Using RF and Optical Wireless Links," *J. Light. Technol.*, vol. 39, no. 22, pp. 7070-7082, 2021.

[29] A. Munari and F. Clazzer, "Modern random access for beyond-5G systems: a multiple-relay ALOHA perspective," in *Proc. BalkanCom*, Skopje, North Macedonia, 2019.

[30] J. G. Andrews, T. Bai, M. N. Kulkarni, A. Alkhateeb, A. K. Gupta, and R. W. Heath, "Modeling and analyzing millimeter wave cellular systems," *IEEE Trans. Commun.,* vol. 65, no. 1, pp. 403–430, 2017.

[31] L. G. Roberts, "ALOHA packet system with and without slots and capture," *ACM SIGCOMM Comput. Commun. Rev.*, vol. 5, no. 2, pp. 28–42, 1975.

[32] I. Gradshteyn and I. Ryzhik, *Table of integrals, series, and products*, 5th ed. San Diego, CA, USA: Academic, 1994.

[33] H. Chen, F. Yin, W. Huang, M. Liu, D. Li, "Ocean surface drifting buoy system based on UAV-enabled wireless powered relay network," *Sensors*, vol. 20, no. 9, 2020.

[34] M. K. Simon and M.–S. Alouni, "Digital Communication over Fading Channels," *John Wiley & Sons*, vol. 95, 2004.